

Research Article

Performance-Driven Symbol Mapping for Downlink and Point-to-Point MIMO Systems

C. Masouros¹ and E. Alsusa²

¹ School of Electrical Engineering, Electronics & Computer Science, Queen's University Belfast, Belfast BT3 9DT, UK

² School of Electrical & Electronic Engineering, University of Manchester, P.O. Box 88, Manchester M601QD, UK

Correspondence should be addressed to C. Masouros, c.masouros@qub.ac.uk

Received 25 October 2010; Revised 10 January 2011; Accepted 18 February 2011

Academic Editor: Rodrigo C. De Lamare

Copyright © 2011 C. Masouros and E. Alsusa. This is an open access article distributed under the Creative Commons Attribution License, which permits unrestricted use, distribution, and reproduction in any medium, provided the original work is properly cited.

An adaptive symbol mapping scheme is proposed for single-user point-to-point and multiuser downlink multiple-input multiple output (MIMO) systems aiming at the minimization of the overall system bit error rate. The proposed scheme introduces a disorder to the symbols to be transmitted within a MIMO subframe by means of dynamic mapping, with the objective to optimise the interference between them and enhance the received symbols' power. This is done by either changing the allocation order of the symbols to the antennas or by applying a scrambling process that alters the symbols sign. This procedure is targeted to optimizing, rather than strictly minimizing the interference between the symbols such that constructive instantaneous interference is utilized in enhancing the decision variables at the receiver on a symbol-by-symbol basis so that detection is made more reliable. In this way, the overall system performance is improved without the need to raise the transmitted power. The proposed scheme can be used in conjunction with various conventional MIMO precoding and detection techniques. The presented results show that for a given transmit power budget this scheme provides significant benefits to the corresponding conventional system's error rate performance.

1. Introduction

The recent advances in multiple-input multiple-output (MIMO) processing [1] are making the application of multiantenna transmitters and receivers increasingly popular in modern wireless communications due to the enhanced capacity and space diversity they offer. MIMO schemes have recently been incorporated in communication standards such as WiMAX and 3GPP-LTE to satisfy the growing demand for higher data rates and quality of service for multimedia applications. Despite the increased information capacity offered by the MIMO channel, the spatial correlation of the multiple subchannels introduces an additional source of interference which corrupts the data symbols and in effect degrades the achievable error rate performance of such systems. In the MIMO uplink, space diversity detection techniques [2–5] can counteract this impediment to a satisfactory extent. In [2, 3], the sphere decoder is presented for an arbitrary lattice code and a lattice code

resulting from applying algebraic space-time coding on a MIMO system, respectively. Regardless of the technique's near-optimal performance, the decoding complexity is quite significant, which makes it impractical for use in mobile units at downlink and point-to-point reception. Suboptimal solutions with reduced complexity are introduced in [4, 5] where diagonal- and vertical-layered architectures of the (Bell Laboratories Layered Space Time) BLAST receiver are presented, respectively. While complexity is drastically reduced the performance of these techniques is comparable to the sphere decoder in most practical scenarios. An alternative to MIMO detection is to shift the signal enhancement processing to the transmitter by use of precoding. This is particularly popular in MIMO downlink communications and point-to-point systems, which is the focus of this work. Channel inversion (CI) [6] entails the least complexity of the precoding techniques available. However, the disadvantages of the CI technique include a poor symbol error rate (SER) performance and the fact that the transmission rate and

throughput delivered are limited and do not improve by increasing the number of antennas, as demonstrated in [7]. The solution proposed in [7], which is a minimum mean square error (MMSE) form of channel inversion, provides some performance and capacity gains with respect to the conventional CI, without a considerable complexity increase. Nevertheless, the transmission rates offered by both these schemes are far from reaching the theoretical channel capacity. Dirty paper coding (DPC) techniques as, for example, in [8–11] based on the initial information theoretical analysis in [12], can further increase transmission rates and achieve significant capacity benefits. However, the majority of the DPC methods developed so far are impractical in many scenarios as they require sophisticated signal processing at the transmitter with complexity similar to the one of sphere decoding. A promising alternative is the joint transmit-receive beamforming scheme as presented in [13] amongst others in the literature. Despite being less complex than DPC, the most robust beamforming schemes require iterative communication between the transmitter and receiver for the optimization of the joint processing and the system configuration. This needs to be done every time the channel characteristics change and hence, in fast fading environments introduces considerable latency to the MIMO downlink system. Owing to their favourable performance-to-complexity tradeoff amongst the techniques mentioned above, this paper focuses on the application of the proposed scheme to the more practical V-BLAST detection and MMSE precoding.

Complementary to the aforementioned signal enhancement processing MIMO schemes, a number of resource allocation schemes [14–19] have emerged for MIMO communications mainly involving antenna selection [14–16] and power allocation [17, 18] for multielement transceivers as well as frequency (subcarrier) allocation [19] for MIMO-orthogonal frequency division multiplexing (OFDM) communications. All the relevant resource allocation methods focus on the reduction of interference between the spatial streams of the MIMO channel. This clearly differentiates them to the proposed scheme where the aim is not strictly to minimise the correlation of the spatial streams but rather to optimise it and accommodate for constructive interchannel interference (ICI). Moreover, resource allocation schemes such as antenna selection can be used in addition to the proposed technique to further improve the performance. The focus of this paper, however, is on signal enhancement schemes and for reasons of coherence, antenna selection and power allocation are not considered here.

In more detail, the proposed scheme which parallels the ones in [20, 21] proposed for code division multiple access (CDMA) is based on the fact that ICI is separated into constructive and destructive as discussed in detail in [22]. The characterisation of the instantaneous ICI depends on the channel characteristics and the correlation between the spatial streams, and, equally importantly, on the instantaneous values of the transmitted symbols. By perturbing the data symbols to be transmitted by means of reordering or scrambling, the proposed scheme influences the ICI between the MIMO subchannels. It then chooses

a symbol mapping such that the interference is optimised and the decision variables at the receiver are maximised. Subsequently, conventional precoding or detection can be applied with enhanced performance due to the optimisation of interference achieved by the proposed symbol mapping.

It is clear that the proposed symbol mapping scheme can be combined with various conventional MIMO detection (linear detection, V-BLAST, sphere decoding, etc.) and precoding schemes (linear precoding, dirty paper coding etc.) to improve the respective performance. For reasons of simplicity and to maintain the focus of the present paper, as mentioned above, only two of the most practical and popular MIMO techniques are considered here, MMSE precoding and V-BLAST detection.

It should be noted that the proposed data allocation method entails the transmission of control signalling (CS) to inform the receiver about the mapping process used so as to attain the correct initial order or appropriately descramble the received data after detection. It will be shown that the CS increases logarithmically with the number of candidate mapping patterns and for this reason the number of possible reordered or scrambled versions of the data to select from should be limited. In the simulations presented here this number is limited to values such that the overhead imposed by the CS transmission is restricted to less than 6% of the transmitted information.

2. System Model and Conventional MIMO Processing

This paper considers transmission in a MIMO system with a limited number of N transmit (Tx) and M receive (Rx) antennas over a frequency flat fading channel. As commonly suggested in the literature, the received signals of all antennas for the i th symbol period can be combined in an $M \times 1$ vector

$$\mathbf{r}^{(i)} = \mathbf{H} \cdot \mathbf{x}^{(i)} + \mathbf{w}^{(i)}. \quad (1)$$

Here $\mathbf{r}^{(i)} = [\mathbf{r}_1^{(i)}, \mathbf{r}_2^{(i)}, \dots, \mathbf{r}_M^{(i)}]^T$ and \mathbf{H} is the $M \times N$ matrix that contains the complex frequency flat channel coefficients with the (m, n) th element $h_{m,n}$ being the zero-mean unit-variance channel tap between the n th transmit antenna and the m th receive antenna. Also, $\mathbf{x}^{(i)} = [x_1^{(i)}, x_2^{(i)}, \dots, x_N^{(i)}]^T$ is the $N \times 1$ vector with the symbols transmitted by the N Tx antennas and $\mathbf{w}^{(i)} = [w_1^{(i)}, w_2^{(i)}, \dots, w_M^{(i)}]^T$ is the $M \times 1$ vector of the additive white Gaussian noise (AWGN) components at the M Rx antennas. For reasons of completeness and to introduce the notation used in this paper, the following briefly presents the conventional MMSE precoding and V-BLAST detection schemes. A modification to the conventional V-BLAST is also introduced to make it more compatible with the proposed method.

2.1. Linear Minimum Mean Square Error (MMSE) Precoding. The MMSE precoding shown in [7] applies a regularized inversion of the channel matrix at the transmitted symbols such that the signal to interference plus noise ratio (SINR) at

the receiver is maximized. The transmitted symbol vector is given as

$$\mathbf{x}^{(i)} = f \cdot \mathbf{H}^* \cdot (\mathbf{H} \cdot \mathbf{H}^* + a \cdot \mathbf{I})^{-1} \cdot \mathbf{b}^{(i)}, \quad (2)$$

where $\mathbf{b}^{(i)} = [b_1^{(i)}, b_2^{(i)}, \dots, b_N^{(i)}]^T$ is the $M \times 1$ data vector for the i th symbol period, $\mathbf{T} = \mathbf{H}^* \cdot (\mathbf{H} \cdot \mathbf{H}^* + a \cdot \mathbf{I})^{-1}$ is the MMSE-like pseudoinverse of the channel matrix and \mathbf{H}^* denotes the Hermitian transpose of \mathbf{H} . f is a scaling factor that ensures that $E\{\|\mathbf{x}^{(i)}\|^2\} = 1$ and is given as

$$f = \sqrt{\frac{1}{\|\mathbf{T}\|^2}} \quad (3)$$

which derives average normalization of the transmitted power. It can be seen that in this case the channel is not entirely orthogonalized and a certain amount of interference remains. The received symbol vector is given as

$$\mathbf{r}^{(i)} = f \cdot \mathbf{R} \cdot \mathbf{b}^{(i)} + \mathbf{w}^{(i)}, \quad (4)$$

where

$$\mathbf{R} = \mathbf{H} \cdot \mathbf{T} = \mathbf{H} \cdot \mathbf{H}^* \cdot (\mathbf{H} \cdot \mathbf{H}^* + a \cdot \mathbf{I})^{-1} \quad (5)$$

is the equivalent crosscorrelation matrix of the symbols as seen at the receiver. The estimated symbols are retrieved by directly quantizing the received signal

$$\hat{\mathbf{b}}^{(i)} = Q(\mathbf{r}^{(i)}), \quad (6)$$

where $Q(\cdot)$ represents the quantization operation. It is shown in [9] that the value of a that maximizes the received SINR is $a = M\sigma^2$, where σ^2 is the noise variance at the receiver. It is demonstrated that this precoding outperforms full channel inversion in symmetric MIMO systems where $N = M$ such as the ones investigated here.

2.2. Vertical Bell Laboratories Layered Space Time (V-BLAST) Detector and Proposed Modification. The V-BLAST detector proposed in [5] involves iterative detection and cancellation of the interfering symbols at each antenna in order to attain an interference-free detection of the desired signal. No precoding is applied at the transmitter ($\mathbf{T} = \mathbf{I}$) and hence $\mathbf{x}^{(i)} = \mathbf{b}^{(i)}$ as the cancellation process is applied on the received signal $\mathbf{r}^{(i)}$ of (1). The function of the scheme is well explained in [5] and for reasons of completeness we present the compact recursive procedure of the technique:

Initialisation:

$$\begin{aligned} m &= 1, \\ \mathbf{G}_m &= (\mathbf{H} \cdot \mathbf{H}^* + \sigma^2 \cdot \mathbf{I})^{-1} \cdot \mathbf{H}^*. \end{aligned} \quad (7a)$$

Recursion:

$$k_m = \arg \min_u \left\| \left[\mathbf{G}_m^T \right]_u \right\|^2, \quad (7b)$$

$$\mathbf{g}_{k_m} = \left[\mathbf{G}_m^T \right]_{k_m}, \quad (7c)$$

$$\hat{b}_{k_m}^{(i)} = Q(\mathbf{g}_{k_m} \cdot \mathbf{r}_m^{(i)}), \quad (7d)$$

$$\mathbf{r}_{m+1}^{(i)} = \mathbf{r}_m^{(i)} - \hat{b}_{k_m}^{(i)} \cdot [\mathbf{H}]_{k_m}, \quad (7e)$$

$$\begin{aligned} \mathbf{G}_{m+1} &= \left(\mathbf{H}_{\bar{k}_m} \cdot \mathbf{H}_{\bar{k}_m}^* + \sigma^2 \cdot \mathbf{I} \right)^{-1} \cdot \mathbf{H}_{\bar{k}_m}^*, \\ m &= m + 1. \end{aligned} \quad (7f)$$

Here $[\mathbf{Y}]_u$ denotes the u th column if \mathbf{Y} is a matrix or the u th element if \mathbf{Y} is a vector, \mathbf{Y}^T denotes the transpose of \mathbf{Y} , k_m denotes the index of the selected symbol to be detected and cancelled at the m th recursion and \hat{b}_{k_m} is the k_m th estimated symbol. In (7e), the estimated interference from symbol b_{k_m} is regenerated using channel state information (CSI) and canceled out from the received signal. In (7f) the rows k_1 to k_m are zeroed in the channel matrix to provide $\mathbf{H}_{\bar{k}_m}$ on which the new equalization matrix \mathbf{G}_{m+1} is based. It is important to stress that in the recursive detection-reconstruction-cancellation part, the m th symbol to be cancelled is selected as the one that corresponds to the row in \mathbf{G}_m with the minimum norm. This is done so that the increase in noise power due to multiplication with \mathbf{g}_{k_m} at each recursion is minimized. However, for the pairing of V-BLAST with the proposed scheme the simulations showed that a criterion based on the one proposed for successive interference cancellation (SIC) in code division multiple access (CDMA) systems in [23] is more appropriate. Therefore in the simulations shown below the received signal is multiplied with the entire equalization matrix at each recursion and the symbol with the highest norm (most reliable for detection) is selected for cancellation at each iteration of the algorithm. Hence, while the conventional V-BLAST is simulated in the graphs below using the procedure in (7a)–(7f) for the combined V-BLAST and symbol mapping the BLAST algorithm is modified to:

Initialisation:

$$m = 1, \quad (8a)$$

$$\mathbf{G}_m = (\mathbf{H} \cdot \mathbf{H}^* + \sigma^2 \cdot \mathbf{I})^{-1} \cdot \mathbf{H}^*.$$

Recursion:

$$\hat{\mathbf{d}}_m^{(i)} = \mathbf{G}_m \cdot \mathbf{r}_m^{(i)}, \quad (8b)$$

$$k_m = \arg \max_u \left\| \left[\hat{\mathbf{d}}_m^{(i)} \right]_u \right\|^2, \quad (8c)$$

$$\hat{b}_{k_m}^{(i)} = Q\left(\left[\hat{\mathbf{d}}_m^{(i)}\right]_{k_m}\right), \quad (8d)$$

$$\mathbf{r}_{m+1}^{(i)} = \mathbf{r}_m^{(i)} - \hat{b}_{k_m}^{(i)} \cdot [\mathbf{H}]_{k_m}, \quad (8e)$$

$$\begin{aligned} \mathbf{G}_{m+1} &= \left(\mathbf{H}_{\bar{k}_m} \cdot \mathbf{H}_{\bar{k}_m}^* + \sigma^2 \cdot \mathbf{I} \right)^{-1} \cdot \mathbf{H}_{\bar{k}_m}^*, \\ m &= m + 1. \end{aligned} \quad (8f)$$

As regards the equalized symbols to be detected in (8b) assuming perfect cancellation the expression can be transformed using (8f) to

$$\begin{aligned}\hat{\mathbf{d}}_m^{(i)} &= \left(\mathbf{H}_{\bar{k}_m} \cdot \mathbf{H}_{\bar{k}_m}^* + \sigma^2 \cdot \mathbf{I} \right)^{-1} \cdot \mathbf{H}_{\bar{k}_m}^* \cdot \mathbf{H}_{\bar{k}_m} \cdot \mathbf{b}_m^{(i)} + \boldsymbol{\eta}_m^{(i)} \\ &= \mathbf{R}_m \cdot \mathbf{b}_m^{(i)} + \boldsymbol{\eta}_m^{(i)},\end{aligned}\quad (9)$$

where \mathbf{R}_m is the crosscorrelation of the remaining symbols at the m th cancellation iteration, and $\boldsymbol{\eta}_m^{(i)}$ is the noise component after channel equalization. It can be proven that the noise component $\boldsymbol{\eta}_m^{(i)}$ has on average increased power compared to $\mathbf{w}_m^{(i)}$ after multiplication with the nonunitary channel equalization matrix.

3. Proposed Optimized Symbol Allocation (SA)

In both (4) and (9) it can be seen that when the transmitted data symbols are reordered they are paired with different crosscorrelation elements in the crosscorrelation matrix and the interference between them changes so that the values of the resulting decision variables are different. Hence, instead of transmitting the symbols $\mathbf{b}^{(i)}$ as they appear at the output of the information source, it would be beneficial to the communication system to reorder the symbols in a way that the decision variables resulting from (4) and (9) are enhanced. This serves as the motivation behind the proposed SA scheme, the flow diagram of which is illustrated in Figure 1. The proposed algorithm involves the following steps.

- (1) From an initial reference symbol-to-antenna allocation pattern a limited number of D candidate allocation patterns are formed offline, known both to the transmitter and receiver. The value of D should be limited, so that the CS bits (needed to convey which of the D candidates was used to the receiver) do not impose an overwhelming transmission overhead.

Transmitter

- (2) For each candidate the expected decision variables are preestimated according to the signal enhancement mechanism employed (precoding or detection). For the MMSE and V-BLAST techniques considered here the preestimated symbols are given by (6) and (8d), respectively using the channel estimates. The vectors containing the decision variables for each candidate allocation are stacked to form the $M \times D$ matrix $\tilde{\mathbf{b}}^{(i)}$. The p th column of the matrix, denoted as $\tilde{\mathbf{b}}_p^{(i)}$ for simplicity, contains the preestimated decision variables for the p th candidate symbol allocation with $p \in \{1, 2, \dots, D\}$.
- (3) A symbol allocation p_{opt} is selected based on an error rate minimization criterion that will be shown in the following.
- (4) The transmitter subsequently allocates the symbols to the antennas based on the selected allocation and, if applicable, precodes the data using some form of conventional precoding.

- (5) Additional to the data symbols the transmitter sends the CS bits that inform the receiver which of the candidate allocation patterns was used.

Receiver

- (6) The receiver applies the conventional signal enhancement processing which can be V-BLAST (assumed in this paper) or any other conventional detection scheme to acquire the enhanced decision variables.
- (7) The CS is detected to determine the allocation p_{opt} used at the transmitter.
- (8) Using the knowledge of all possible allocation patterns, the receiver then removes the perturbation introduced at the transmitter by inverting the process of p_{opt} to retrieve the original data.

For reasons of clarity the separation between the notations $\tilde{\mathbf{b}}^{(i)}$ and $\hat{\mathbf{b}}^{(i)}$ in the above analysis should be emphasized, as the former represents the preestimated values of the data at the transmitter using CSI and ignoring noise while the latter denotes the actual estimated data at the receiver.

It is evident that for each allocation pattern used, a number of $c = \lceil \log_2(D) \rceil$ control signaling bits need to be transmitted additionally to the information symbols to notify the receiver which of the D candidate allocations was selected. Therefore if the proposed SA was applied at individual symbol periods, in realistic MIMO scenarios with limited number of antennas the need to map the symbols at each symbol period would yield a significant amount of CS. To limit the signaling overhead to practical levels, rather than applying the proposed SA on a symbol-by-symbol basis, symbols of multiple transmission time slots and spatial layers are grouped to form MIMO subframes, similar to the ones used in the LTE standard. By applying SA on these subframes and increasing the number of data information symbols per allocation the relative CS overhead is dramatically reduced.

As regards the mapping mechanism used to create the D candidate allocations and introduce the diversity in the resulting interference to optimize the decision variables, this paper proposes two distinct methods which are analyzed below.

3.1. Mapping Method 1: Symbol Reordering. The symbols within the MIMO subframe are randomly shuffled to produce a reordered version of the data subframe as shown in Figure 2(a). This can be expressed by the mapping operation

$$\left[\mathbf{b}_p^{(i)} \right]_k = \left[\mathbf{b}^{(i)} \right]_{l_p^k} \quad (10)$$

for the p th candidate allocation. Here l^p is the p th randomly permuted sequence of positive integer indexes of 1 to L , where L is the total number of symbols per subframe. For the example of $L = 5$, three possible permutations could be $l^1 = [3, 1, 5, 4, 2]$, $l^2 = [2, 4, 1, 5, 3]$, and $l^3 = [5, 3, 4, 1, 2]$. Assuming the permutation l^1 , (10) denotes that $\left[\mathbf{b}_p^{(i)} \right]_3 = \left[\mathbf{b}^{(i)} \right]_5$. Clearly, $\mathbf{b}_p^{(i)}$ is a space-time reordered version of $\mathbf{b}^{(i)}$ which is used to preestimate the decision

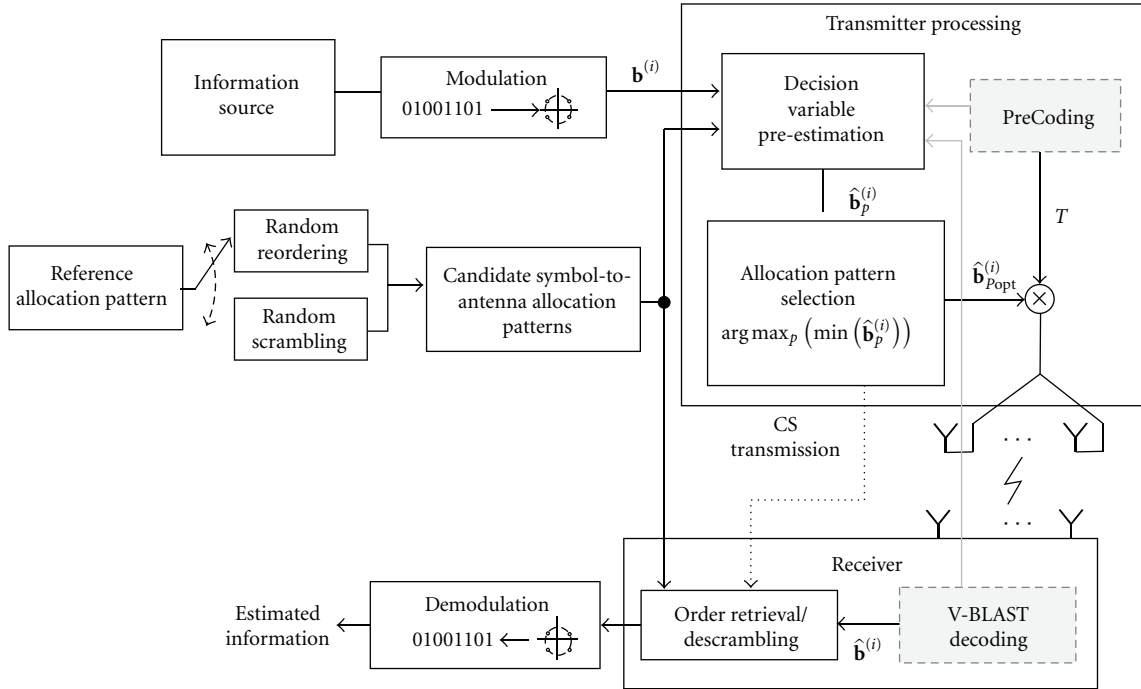


FIGURE 1: Block diagram of the proposed symbol allocation (SA) scheme.

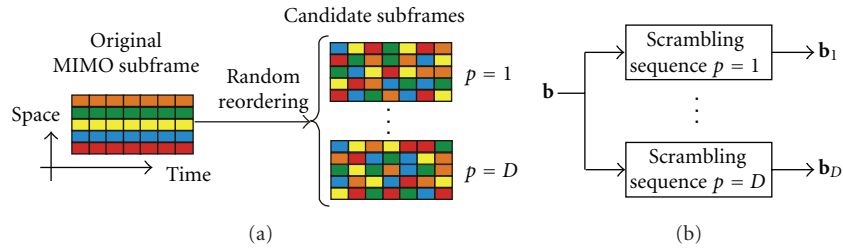


FIGURE 2: Mapping methods: (a) symbol reordering, (b) symbol scrambling.

variables for the given candidate allocation. Any individual symbol within the subframe can be transmitted at any spatial layer or time slot within the subframe. This means that the corresponding symbol can be received at any time slot and more importantly at any receive antenna. Therefore the receive antennas need to cooperate to reestablish the actual order of the data in order for them to be used for the intended application. Hence, the usefulness of this form of perturbation is limited to point-to-point MIMO systems. If the length of the subframe is a number of N_t time slots then the number of symbols reordered for a transmitter with N antennas is $L = N \cdot N_t$. For a number of $L = N \cdot N_t$ symbols to be shuffled there exists a number of

$$F_r = (N \cdot N_t)! \quad (11)$$

different reordered versions of the subframe. Nevertheless as mentioned in the previous section the number of candidate allocation patterns needs to be limited $D \ll F_r$ in order to restrict the resulting CS overhead. It will be shown however in the results section that the performance benefit provided

by SA, while less than the theoretically achievable for $D = F_r$, is still considerable compared to conventional MIMO schemes.

3.2. Mapping Method 2: Symbol Scrambling. The symbols within the MIMO subframe are randomly scrambled as shown in Figure 2(b), so that the sign (but not the absolute value) of the real and imaginary parts of the symbols existing in the subframe change. This can be expressed by the element wise multiplication of the data symbols with a scrambling sequence \mathbf{s}_p

$$\mathbf{b}_p^{(i)} = \mathbf{s}_p \circ \mathbf{b}^{(i)}, \quad (12)$$

where $\mathbf{s}_p = [s_p^1, s_p^2, \dots, s_p^L]$ has elements of the form $s_p^k = \{\pm 1, \pm i\}$. In this case the initial order of the time slot and spatial stream allocated to the symbols from the information source is unchanged but the actual symbol value is altered in favor of constructive instantaneous interference. Similar to conventional scrambling techniques, a scrambling

sequence is applied on the group of symbols to introduce the desirable interference diversity. In contrast to conventional scrambling however, the aim is to constructively correlate the symbols rather than fully decorrelate them. For the example of quadrature phase shift keying (QPSK) used in the following simulations a complex scrambling code needs to be employed. Since with random scrambling each symbol can take any of the four different values in the QPSK constellation, for the number of $L = N \cdot N_t$ symbols in the subframe there exist

$$F_s = 4^{(N \cdot N_t)} \quad (13)$$

different possible scrambled versions. It will be shown however that the performance of the proposed scheme depends on the number of actual candidate perturbed versions of the frame rather than the theoretical achievable diversity. Therefore for a practical number of candidate allocations $D \ll F_r, F_s$ the performances of the two mechanisms are identical as shown in the simulations that follow. The advantage of the scrambling method however lies in the fact that since the symbols arrive at the receive antennas at the initial time slots and spatial streams there is no need for the antennas to cooperate for retrieving the actual order of the transmitted data. This makes the proposed scheme also applicable to multiuser MIMO downlink transmission.

4. Selection of the Symbol Allocation

4.1. Selection Criterion. From (4) and (9), a number of criteria can be formulated for the selection of the symbol allocation to be used for transmission based on the resulting interference and decision variables for each candidate allocation pattern. Since the average error rate performance of a point-to-point MIMO system is governed by the performance of the instantaneously “worst” symbols we propose to select the allocation pattern that derives the decision variable distribution with the most reliable worst symbol. The obvious choice would be to select the allocation according to a Euclidean distance criterion

$$p_{\text{opt}} = \arg \min_p \left(\max_k \left\| \left[\tilde{\mathbf{b}}_p^{(i)} \right]_k - \left[\mathbf{b}_p^{(i)} \right]_k \right\| \right), \quad (14)$$

$$p \in \{1, 2, \dots, D\},$$

that is, select the allocation that minimizes the maximum Euclidean distance to the data symbols (worst symbol) in the preestimated symbol distribution. However, this does not allow for constructive interference which pushes the received symbols further away from the nominal constellation points, towards the direction opposite from the decision thresholds. This is shown graphically in Figure 3 for the example of constellation point $x = 1 + j$ of the QPSK constellation. It can be seen that although the received symbol denoted by “+” has a smaller Euclidean distance to x than the point denoted by “o”, the latter has increased distances to the decision thresholds of the QPSK constellation (the real and imaginary axes) and therefore is more tolerant to noise and yields more reliable detection. For this reason the proposed criterion is

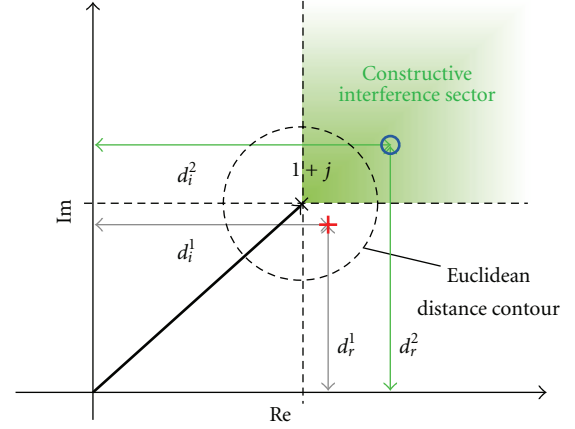


FIGURE 3: Euclidean distance versus projection criterion, QPSK $x = 1 + j$ example.

based on the projection of the preestimated symbols on the data symbols, which for phase shift keying (PSK) modulation is expressed as

$$p_{\text{opt}} = \arg \max_p \left(\min \left(\left[\tilde{\mathbf{b}}_p^{(i)} \circ \mathbf{b}_p^{(i)} \right]_k \right) \right), \quad p \in \{1, 2, \dots, D\}. \quad (15)$$

Here $\tilde{\mathbf{b}}_p^{(i)} \circ \mathbf{b}_p^{(i)}$ denotes the projection of the elements of vector $\tilde{\mathbf{b}}_p^{(i)}$ to the elements of vector $\mathbf{b}_p^{(i)}$ for the p th allocation pattern. For the case of binary PSK (BPSK) the projection involves the element wise multiplication of the two vectors while for QPSK the real and imaginary parts of the elements need to be separated prior to element wise multiplication

$$\left[\tilde{\mathbf{b}}_p^{(i)} \circ \mathbf{b}_p^{(i)} \right]_k = \text{Re} \left[\tilde{\mathbf{b}}_p^{(i)} \right]_k \cdot \text{Re} \left[\mathbf{b}_p^{(i)} \right]_k + j \cdot \text{Im} \left[\tilde{\mathbf{b}}_p^{(i)} \right]_k \cdot \text{Im} \left[\mathbf{b}_p^{(i)} \right]_k. \quad (16)$$

When the projection of the preestimated decision variable on the actual symbol to be transmitted is negative it signifies that due to ICI the decision variable is corrupted and would indicate a different constellation point than the one transmitted which would lead to erroneous detection. When the projection is positive the ICI does not push the decision variable to a different constellation point and in the absence of noise detection is expected to be successful. The higher the value of the projection the more reliable the decision variables are expected to be. Hence the minimum of the projection for each candidate $\min(\tilde{\mathbf{b}}_p^{(i)} \circ \mathbf{b}_p^{(i)})$ denotes the most unreliable (worst) symbol in the distribution $\tilde{\mathbf{b}}_p^{(i)}$. By selecting the candidate allocation with the highest minimum projection for every subframe the performance of the instantaneously worst symbol is constantly enhanced and therefore the overall average performance is boosted.

To verify the superiority of the proposed criterion over the conventional approach, the two criteria (14) and (15) are compared in the results that follow. It should be noted that since the search for the best candidate is not exhaustive amongst all possible perturbed symbol allocations but rather

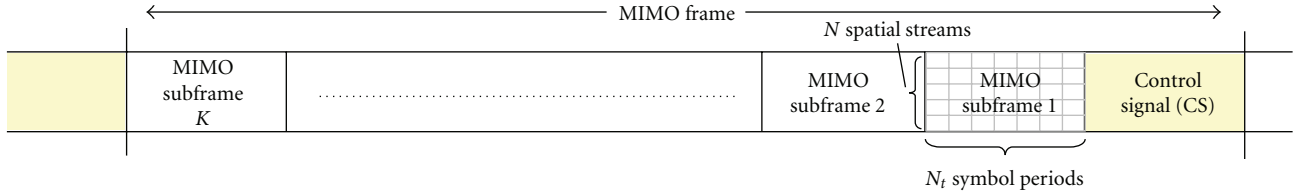


FIGURE 4: Proposed frame structure.

between $D \ll F_r, F_s$ possibilities—to limit the CS—the selected candidate may be suboptimum. It is shown in the simulations however that even for this suboptimal selection a significant performance improvement can be gleaned.

4.2. Selection Implementation. As regards the selection of p_{opt} , the obvious method for this is to calculate p_{opt} in (15) for each symbol period. An alternative would be to calculate p_{opt} for all symbol combinations for a given channel impulse response and store the values of p_{opt} in a memory, possibly in the form of a lookup table (LUT). For each symbol period the transmitter would then select the appropriate value of p_{opt} from the LUT according to the symbol combination encountered. For QPSK modulation and $N = 5$ assumed in the following results the number of possible symbol combinations would be $\beta = 4^N = 1024$. However, for PSK modulation the interference encountered depends only on the relative phases of the data symbols and not their amplitudes which are common for all constellation points. Hence different data symbol combinations that share the same relative phases such as $\mathbf{b}^{(i)} = [1+j, 1-j, -1-j, -1+j, 1+j,]$ and $\mathbf{b}^{(i)} \cdot e^{j\pi} = [1-j, -1-j, -1+j, 1+j, 1-j,]$ would yield the same value of p_{opt} . Clearly there exist $\beta_0 = \beta/4 = 256$ relative phase combinations arising from each of the QPSK constellation points. Hence, a total number of $\beta_0 = 4^{N-1}$ entries need to be calculated and stored in the LUT. This LUT-based implementation of the allocation selection is particularly preferable in slow fading cases where the channel coefficients remain unchanged for large numbers of symbol periods and large framelengths $B \gg \beta_0$ can be used.

5. Control Signalling (CS) and Resulting Transmission-Reception Efficiency

5.1. CS Transmission. It is evident from the aforementioned analysis that the performance of the proposed scheme relies on the transmission of CS to update the receiver on the allocation pattern used at each symbol period in order to correctly remove the perturbation introduced at the transmitter and obtain the initial data. It is possible to attach the CS at the end of the corresponding subframe but for reasons of efficiency it is preferable to adopt a frame-based approach as the one shown in Figure 4. The MIMO frame consists of K subframes each one comprising N_t symbol periods over N spatial streams. The CS is calculated for the whole MIMO frame and is transmitted at the beginning of the frame. This facilitates the perturbation removal at the

receiver as the whole frame can be processed uniformly in order to avoid subframe-by-subframe CS transmission and detection. The CS is transmitted separately to the data to avoid interference so that CS detection is reliable.

5.2. CS Transmission-Reception Efficiency. As mentioned above a number of D candidate allocations can be represented using $c = \lceil \log_2(D) \rceil$ bits. Assuming M_0 -ary modulation for the CS, a number of $s = \lceil \log_2(D) \rceil / \log_2(M_0)$ CS symbols need to be transmitted for every switch of the allocation pattern, while when the allocation pattern is constant, no CS is transmitted. Assuming the worst case where the pattern is changed at each subframe, a number of s CS symbols needs to be transmitted for every $L = N \cdot N_t$ transmitted data symbols in the subframe and therefore the transmission efficiency can be expressed as

$$\mathcal{E} = \frac{N \cdot N_t}{N \cdot N_t + \lceil \log_2(D) \rceil / \log_2(M_0)}. \quad (17)$$

Likewise, at the receiver a number of s CS symbols need to be detected for every $L = N \cdot N_t$ received data symbols which gives an equal reception efficiency. In the majority of the following simulations a data subframe of $N_t = 7$ symbol periods over $N = 5$ spatial streams is assumed and a number of $D = 16$ candidate allocations is used. As QPSK modulation is employed for both data and CS this derives a practical transmission and reception efficiency of $\mathcal{E} = 94.6\%$. At this point it should be mentioned that a 5.4% efficiency reduction, while nontrivial, is worthwhile due to the significant performance improvement attained by the proposed scheme. Indeed, it is not uncommon to sacrifice a degree of transmission efficiency to secure performance benefits and a profound example of this is forward error correction (FEC) coding. While it imposes major transmission overheads such as 33% for codes of rate $\mathcal{R} = 3/4$, 100% for rate $\mathcal{R} = 1/2$ and so on, it greatly improves communications system performance. This is why FEC is adopted in most modern communication standards and its importance is widely acknowledged. Furthermore, the transmission efficiency of the proposed scheme in (17) can be improved by increasing M_0 and employing higher-order modulation such as 16-quadrature amplitude modulation (QAM) or 64QAM. This is further illustrated in Figure 7 (and the relevant discussion in the following) which plots the transmission efficiency with increasing D for the parameters mentioned above and for various modulation schemes used for the CS transmission.

TABLE 1: Complexity in numbers of operations for MMSE and MMSE-SA.

MMSE		No. of operations	MMSE-SA		No. of operations
(1)	construct \mathbf{R}	$O(N \cdot M^2)$	(1)	construct \mathbf{R}	$O(N \cdot M^2)$
(2)	invert \mathbf{R}	$O(M^3)$	(2)	invert \mathbf{R}	$O(M^3)$
(3)	multiply \mathbf{R}^{-1} with \mathbf{H}^*	$O(N \cdot M^2)$	(3)	multiply \mathbf{R}^{-1} with \mathbf{H}^*	$O(N \cdot M^2)$
(4)	multiply with $\mathbf{b}^i \times N_t$	$N_t \cdot O(N \cdot M)$	(4)	multiply with $\mathbf{b}_p^{(i)} \times N_t \times D$	$N_t \cdot D \cdot O(N \cdot M)$
(5)	calculate scaling factor	$O(M)$	(5)	calculate scaling factor	$O(M)$
			(6)	choose optimum $\mathbf{b}_p^{(i)} \times N_t$	$N_t \cdot D \cdot O(N)$
Total	$O(M^3) + 2 \cdot O(N \cdot M^2) + N_t \cdot O(N \cdot M) + O(M)$		Total	$O(M^3) + 2 \cdot O(N \cdot M^2) + O(M) + N_t \cdot D \cdot [O(N \cdot M) + O(N)]$	

6. Complexity Analysis

In order to investigate the complexity repercussions of the above methodology, the relevant comparison of the conventional and proposed techniques is illustrated in Table 1. The table illustrates the complexity of conventional MMSE precoding with MMSE using symbol allocation (MMSE-SA). The complexity count is shown in terms of principal factors $O(\cdot)$ as commonly done in the literature. A slow fading channel is assumed where the channel estimates and the precoding matrix need to be updated once every MIMO frame. It can be seen that for the proposed scheme the principal complexity factor is the need to trial between all candidate symbol allocations at the transmitter before selection. This increases the vector ($\mathbf{b}_p^{(i)}$) to matrix (\mathbf{T}) multiplications by a factor equal to the number of candidate allocations D . The resulting complexity increase relative to conventional MMSE can be expressed as

$$\frac{(N_t - 1) \cdot D \cdot O(N \cdot M) + N_t \cdot D \cdot O(N)}{O(M^3) + 2 \cdot O(N \cdot M^2) + N_t \cdot O(N \cdot M) + O(M)}. \quad (18)$$

For the case of fast fading where channel estimation and precoding matrix calculation (steps 1, 2, 3, 5 in Table 1) need to be done more frequently, the weight of the factor D that relates to the complexity increase for the proposed scheme in (18) is reduced. Therefore, the relative complexity increase for MMSE-SA compared to MMSE is drastically reduced. It should be mentioned that in the cases where the proposed scheme is applied on the MIMO downlink by use of scrambling the discussed complexity increase has less of an impact as it involves the base station transmitter where resources are more affordable. Moreover, by use of the LUT-based approach discussed in Section 4.2) the complexity of the proposed scheme can be further reduced. Overall, the raise in complexity is well justified by the performance benefits provided by the proposed technique as will be shown by the results.

7. Performance Analysis for Nonideal CS Transmission

Another important aspect of the proposed SA scheme is the dependency of its performance on the correct reception of the CS. This issue is treated in this section where a

performance analysis is presented for the case of imperfect CS detection. Assume that P_d is the probability of bit error for the data detection in the case of error-free CS. In the case of erroneous CS detection, the data detection becomes random and the probability of bit error is 1/2. Hence the probability of correct detection per data bit becomes

$$P_s = \begin{cases} \frac{1}{2}, & \text{erroneous CS,} \\ 1 - P_d, & \text{corrects CS.} \end{cases} \quad (19)$$

Also, if P_e is the bit error probability for the CS detection, for a number of c CS bits the probability of correct CS detection becomes $P_c = (1 - P_e)^c$. Following the above, the probability of success in the data detection considering the CS performance is given as

$$P_s = \frac{1}{2} \cdot (1 - (1 - P_e)^c) + (1 - P_d) \cdot (1 - P_e)^c, \quad (20)$$

while the resulting probability of data error per bit for imperfect CS detection is

$$\mathcal{P} = 1 - P_s = \frac{1}{2} + \left(P_d - \frac{1}{2}\right) \cdot (1 - P_e)^c. \quad (21)$$

For M_0 -PSK modulation the error probability per CS bit (P_e) is the flat fading M_0 -PSK bit error probability [24] expressed as

$$P_e = \left(\frac{M_0 - 1}{M_0}\right) \cdot \left\{1 - \lambda \cdot \sqrt{\frac{g \cdot \bar{\gamma}_b}{1 + g \cdot \bar{\gamma}_b}} \left(\frac{M_0}{(M_0 - 1)\pi}\right)\right\}, \quad (22)$$

where $g = \sin^2(\pi/M_0)$,

$$\lambda = \frac{\pi}{2} + \tan^{-1} \left[\sqrt{\frac{g \cdot \bar{\gamma}_b}{1 + g \cdot \bar{\gamma}_b}} \cot(M_0) \right], \quad (23)$$

$$\bar{\gamma}_b = \frac{E_b}{N_0} \cdot E(a_f^2). \quad (24)$$

In (24) a_f is the amplitude of flat fading, E_b is the energy per bit, N_0 is the noise power spectral density and $E(x)$ denotes the expected value of x . The probability of symbol error for QPSK modulation used in the simulations below can

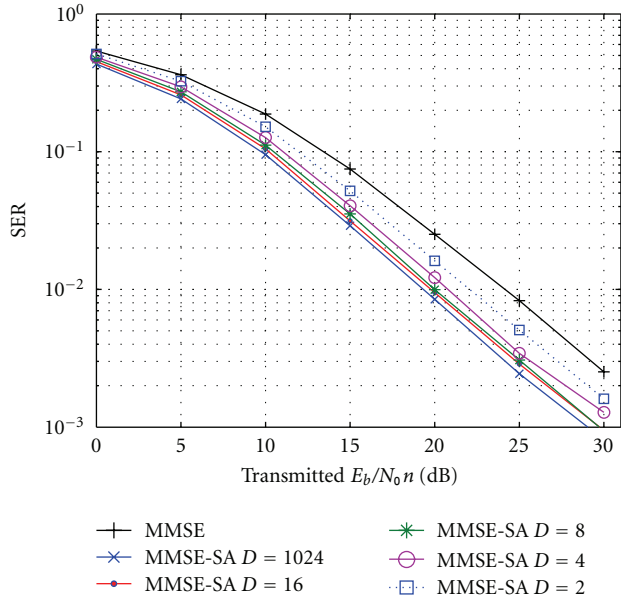


FIGURE 5: SER versus SNR for MMSE, MMSE-SA for increasing D , $N = M = 5$, $N_t = 1$, QPSK.

then be simply calculated using (22) and (23) for $M_0 = 4$. It can be observed that as the signal to noise ratio (SNR) increases and the CS detection becomes more reliable P_e tends to zero for which case (21) yields $\mathcal{P} = P_d$. The value P_d for the proposed SA scheme is dependent on which of the investigated conventional techniques are used and how SA enhances performance. It is obvious that $\mathcal{P} > P_d$ for nonzero P_e , but the following simulations show that with the proposed SA the data detection error probability P_d is severely reduced compared to the corresponding conventional techniques. Hence \mathcal{P} for SA is still significantly less than the error probability of the conventional methods. The exact error probability P_d cannot be calculated in closed form due to the fluctuations in the symbol allocation and the instantaneous crosscorrelation values between the symbols. Therefore, an exact expression of the final error probability \mathcal{P} for imperfect CS detection cannot be derived. Simulation results are provided in the following section for the proof of the proposed method's superiority.

8. Numerical Results

This section presents the results of Monte Carlo simulations carried out for conventional MIMO precoding and detection schemes with and without the proposed SA for various numbers of antennas on frequency flat fading MIMO channels in order to illustrate the relevant performance comparison. While it is intuitive that the benefits of the proposed scheme extend to a variety of MIMO techniques, the simulations below focus on MMSE precoding and V-BLAST detection, as these schemes offer a practical performance-to-complexity tradeoff. For the simulations shown QPSK modulation has been employed and unless stated otherwise perfect channel estimates are assumed. For the transmission of CS an

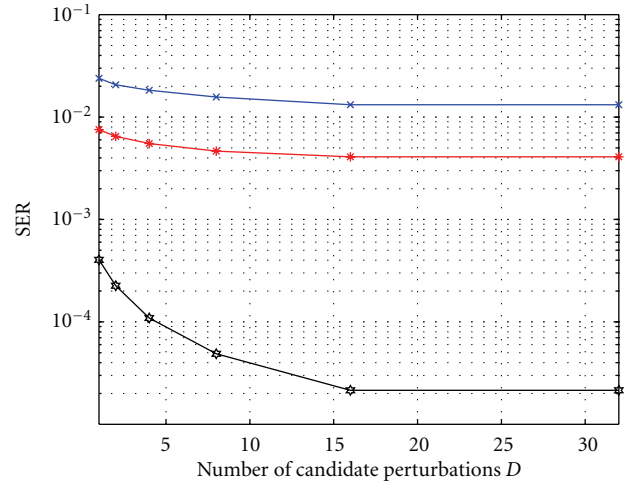


FIGURE 6: SER versus D for MMSE (SNR = 20 dB, 25 dB) and V-BLAST (SNR per rx antenna = 20 dB) using SA, $N = M = 5$, $N_t = 7$, QPSK.

increased transmission power by a factor of two compared to the data transmission is assumed, which is a common method in practical systems to achieve reliable CS and eliminate the effect on data detection. To avoid confusion it should be clarified that to ease comparison to the results of [5, 9] the total transmitted SNR is used in the graphs for MMSE precoding while the values of transmitted SNR per receive (rx) antenna are used in the graphs for V-BLAST detection.

8.1. Reference Achievable Performance Gain. As an initial point and to quantify the absolute performance benefit achievable by SA on MMSE precoding Figure 5 depicts the performance of MMSE-SA on a MIMO symbol rather than on a MIMO subframe basis ($N_t = 1$) for a system with $N = M = 5$. In the results shown here the symbol allocation is optimized at every symbol period and the candidates are increased up to the maximum possible $D = \max(F_r, F_s) = 4^N = 1024$. In realistic scenarios this would impose a significant amount of CS which renders the SA scheme impractical. Hence the result here is shown for reference purposes only, ignoring the need for CS transmission. It can be seen that the benefit achievable for maximum D is almost 5 dB. It is worthwhile to note that drastically decreasing the candidate allocations to $D = 16$ and $D = 8$ imposes only an insignificant performance loss. The performance gain is halved however when $D = 2$.

8.2. Selection of Optimum D and Resulting Transmission-Reception Efficiency. A profound insight of the performance to transmission efficiency tradeoff can be attained by Figures 5 and 6 where the symbol error rate (SER) performance and transmission efficiency are shown for increasing values of D ,

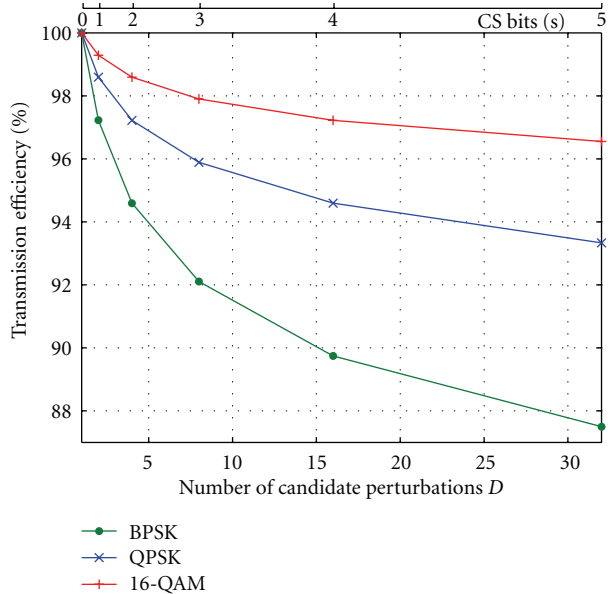


FIGURE 7: Transmission-reception efficiency for SA for increasing D , $N = M = 5$, $N_t = 7$, QPSK.

respectively. The same 5×5 MIMO system is considered but in this case a subframe-based optimization of the symbol allocation is employed as the one analyzed in Section 5. A subframe length of $N_t = 7$ time slots is assumed which derives a number of $L = 35$ data symbols per subframe. In Figure 6 the performance of MMSE precoding is shown for a total transmitted SNR of 20 and 25 dB and the performance of V-BLAST is included for transmitted SNR per antenna of 20 dB. It can be seen that for low values of D the performance gain for increasing D is significant while at higher values of $D = 8$ and $D = 16$ this benefit saturates. Considering the transmission efficiency diagram of Figure 7 and especially the curve for QPSK modulation of the CS bits it can be seen that the reduction in efficiency is considerable between $D = 16$ and $D = 32$. Therefore it can be concluded that for the system investigated in the majority of simulations in this paper, for which $N_t = 7$ and $N = M = 5$, the value of $D = 16$ provides a favorable performance-to-efficiency tradeoff. Hence, unless stated otherwise it is the one used in the following simulations. For this case the relevant transmission-reception efficiency of (17) is $\mathcal{E} = 94.6\%$. It is apparent in Figure 7 that the transmission efficiency can be increased by using 16QAM modulation which for this value of D gives $\mathcal{E} = 97.22\%$ in the graph yielding less than 3% of overhead.

8.3. Further Performance Investigation. The SER versus transmitted SNR performance for MMSE is shown in Figure 8 for the same system of $N = M = 5$, $N_t = 7$. The graph depicts the performance for both mapping mechanisms of Section 3, namely reordering and scrambling and it can be seen that for the same value of D both perform identically. Hence the results confirm that as mentioned above, it is the value of D that makes the difference in performance rather

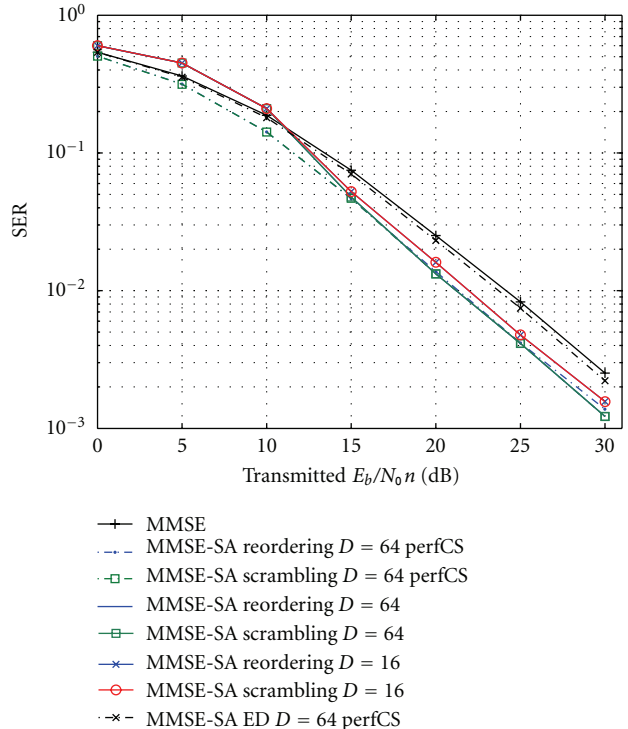


FIGURE 8: SER versus SNR for MMSE, MMSE-SA with reordering or scrambling, projection-based optimisation and MMSE-SA with Euclidean distance (ED) optimisation $N = M = 5$, $N_t = 7$, QPSK.

that the mapping method used. Moreover, to illustrate the superiority of the proposed projection criterion (15) over the Euclidean distance (ED) criterion (14) for the selection of p_{opt} , the performance of the latter is also included for the case of error-free CS. It can be seen that the ED criterion only provides a minimal improvement with respect to the performance of the conventional system, while the existence of constructive interference for the proposed criterion offers a notable improvement. The performance of the system with error-free CS transmission is also depicted for comparison. It can be viewed that the negative impact of the CS transmission on the performance of the system is apparent at low SNR values where CS detection is problematic, while it becomes negligible for higher SNRs where the CS detection is reliable. As a result, for low SNRs the proposed technique is outperformed by conventional MMSE precoding due to the unreliability of the CS transmission. However, for the higher SNR values a considerable SER reduction can be observed which yields a 2 dB gain in the transmitted SNR for $D = 16$ for this 5×5 MIMO system. A 2.5 dB gain can be attained by allowing a reduction of the transmission efficiency using $D = 64$ for the same system.

The performance of V-BLAST is investigated in Figure 9 where the bit error rate (BER) versus SNR per rx antenna is shown. The same MIMO system of $N = M = 5$, $N_t = 7$, $D = 16$ is assumed. Again the performances for both mapping techniques are depicted to validate their equality. The performance of the system with error-free

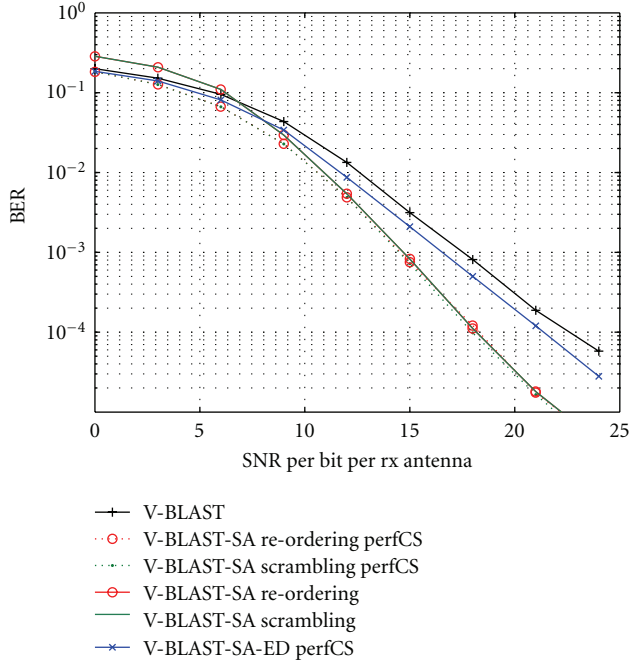


FIGURE 9: BER versus SNR for V-BLAST, V-BLAST-SA with reordering or scrambling, projection-based optimisation and V-BLAST-SA with Euclidean distance (ED) optimisation $N = M = 5$, $N_t = 7$, $D = 16$, QPSK.

CS transmission is also included for comparison and it is obvious that the negative impact of the CS transmission on the performance of the system only exists at low SNR values. At higher values an SNR gain of 5 dB can be viewed for V-BLAST-SA compared to conventional V-BLAST. Notably the BER reduction for SNR = 20 dB is of an order of a magnitude which consists of a worthwhile improvement for this small scale MIMO system. Again the performance of the ED criterion (14) for the selection of p_{opt} , is also shown for comparison. Clearly, the proposed criterion benefits from allowing constructive interference in comparison to the ED criterion.

Figure 10 shows the BER performance for increasing number of antennas for the symmetric ($M = N$) MIMO channel for the case of V-BLAST and V-BLAST-SA. Two sets of results are shown for the cases when the SNR per rx antenna takes the values of 10 dB and 15 dB. It can be seen that for practical values of $N = 2$ to $N = 6$ for point-to-point MIMO systems the proposed scheme considerably improves the performance of the conventional system. One can observe that the BER is improving up to a certain N for both techniques. This is because the SNR per receive antenna is considered here, which for increasing antennas derives increasing total SNR. Therefore the performance naturally increases up to a certain point where the ICI becomes dominant in the system. Overall the proposed scheme outperforms conventional V-BLAST for all values of N .

In all simulations above the CSI is assumed perfectly known at the transmitter. However the processing of the

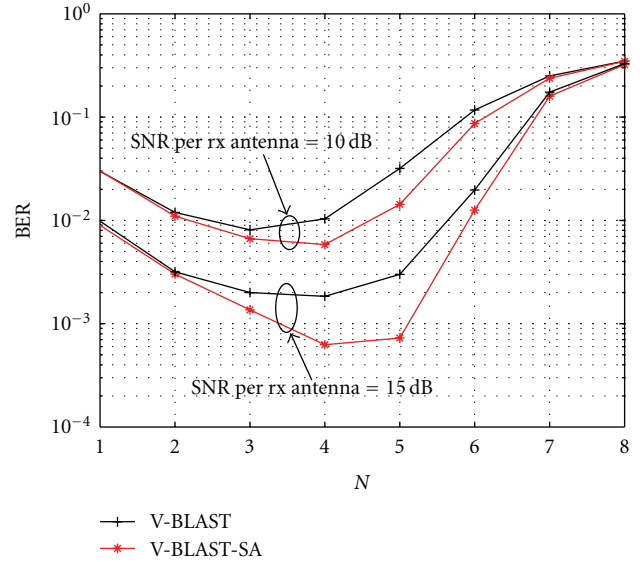


FIGURE 10: BER versus N for V-BLAST, V-BLAST-SA for SNR per rx antenna = 10 dB and 15 dB, $N = M$, $N_t = 7$, QPSK.

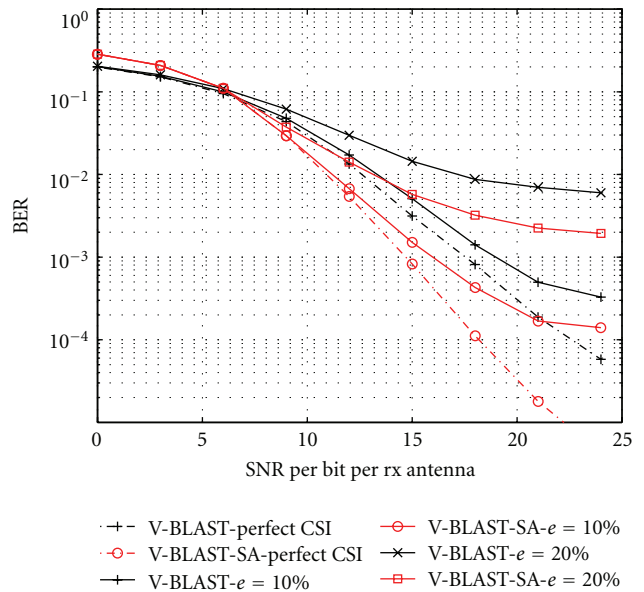


FIGURE 11: BER versus SNR for V-BLAST, V-BLAST-SA for CSI errors $e = 0$, $e = 10\%$, $e = 20\%$, $N = M = 5$, $N_t = 7$, $D = 16$, QPSK.

proposed scheme as shown in Section 3 suggests that SA could be sensitive to CSI errors. To validate the usefulness of the proposed scheme in scenarios with erroneous channel estimates, Figure 11 depicts the BER performance of V-BLAST and V-BLAST-SA for increasing CSI errors. In order to maintain a generic performance comparison irrespective to any channel estimation technique or type of CSI errors,

these errors are simulated by adding a complex random deviation to the channel coefficients available at the transmitter to derive an error in the estimated coefficients of

$$e = \frac{|h_{m,n} - \hat{h}_{m,n}|}{h_{m,n}}. \quad (25)$$

Here $h_{m,n}$ denotes the flat fading channel coefficient between the n th transmit and the m th receive antennas while $\hat{h}_{m,n}$ represents the corresponding channel estimate. Results for $e = 10\%$ and $e = 20\%$ are shown and for reasons of comparison the performance graphs for perfect CSI are retained in the figure. It can be seen that the performance of the proposed V-BLAST-SA degrades in the same way as conventional V-BLAST for increasing CSI errors. In all cases V-BLAST-SA still outperforms conventional V-BLAST for the higher SNR values when CS detection is reliable.

9. Conclusions and Future Work

The use of static data-to-antenna allocation leads to waste of useful energy inherent in the communication channel and makes conventional MIMO schemes suboptimal. By applying adaptive mapping on the data to be transmitted and introducing diversity in the interference between the transmitted symbols of the MIMO channel this work has shown that significant performance benefits are gleaned for MIMO systems. The tradeoff to this improvement is the need for control signaling for the correct data detection. Further work can be carried out towards reducing the CS overhead and applying the proposed scheme to further and more advanced MIMO techniques including resource allocation.

Acknowledgments

This work has been jointly funded by EPSRC and Philips Research Labs, UK. The authors would like to thank Dr. Tim Mousley for the helpful discussions throughout this research contribution.

References

- [1] G. Caire and S. Shamai, "On the achievable throughput of a multiantenna Gaussian broadcast channel," *IEEE Transactions on Information Theory*, vol. 49, no. 7, pp. 1691–1706, 2003.
- [2] E. Viterbo and J. Boutros, "A universal lattice code decoder for fading channels," *IEEE Transactions on Information Theory*, vol. 45, no. 5, pp. 1639–1642, 1999.
- [3] O. Damen, A. Chkeif, and J. C. Belfiore, "Lattice code decoder for space-time codes," *IEEE Communications Letters*, vol. 4, no. 5, pp. 161–163, 2000.
- [4] G. J. Foschini, "Layered space-time architecture for wireless communication in a fading environment when using multi-element antennas," *Bell Labs Technical Journal*, vol. 1, no. 2, pp. 41–59, 1996.
- [5] P. W. Wolniansky, G. J. Foschini, G. D. Golden, and R. A. Valenzuela, "V-BLAST: an architecture for realizing very high data rates over the rich-scattering wireless channel," in *Proceedings of the URSI International Symposium on Signals, Systems, and Electronics (ISSSE '98)*, pp. 295–300, October 1998.
- [6] T. Haustein, C. von Helmolt, E. Jorswieck, V. Jungnickel, and V. Pohl, "Performance of MIMO systems with channel inversion," in *Proceedings of the 55th Vehicular Technology Conference (VTC '02)*, pp. 35–39, Birmingham, Ala, USA, May 2002.
- [7] C. B. Peel, B. M. Hochwald, and A. L. Swindlehurst, "A vector-perturbation technique for near-capacity multiantenna multiuser communication—part I: channel inversion and regularization," *IEEE Transactions on Communications*, vol. 53, no. 1, pp. 195–202, 2005.
- [8] M. Tomlinson, "New automatic equaliser employing modulo arithmetic," *Electronics Letters*, vol. 7, no. 5-6, pp. 138–139, 1971.
- [9] H. Harashima and H. Miyakawa, "Matched-transmission technique for channels with intersymbol interference," *IEEE Transactions on Communications*, vol. 20, no. 4, pp. 774–780, 1972.
- [10] U. Erez, S. Shamai, and R. Zamir, "Capacity and lattice strategies for canceling known interference," *IEEE Transactions on Information Theory*, vol. 51, no. 11, pp. 3820–3833, 2005.
- [11] H. El Gamal, G. Caire, and M. O. Damen, "Lattice coding and decoding achieve the optimal diversity-multiplexing tradeoff of MIMO channels," *IEEE Transactions on Information Theory*, vol. 50, no. 6, pp. 968–985, 2004.
- [12] M. H. M. Costa, "Writing on dirty paper," *IEEE Transactions on Information Theory*, vol. 29, no. 3, pp. 439–441, 1983.
- [13] F. Rashid, K. J. R. Liu, and L. Tassiulas, "Transmit beamforming and power control for cellular wireless systems," *IEEE Journal on Selected Areas in Communications*, vol. 16, no. 8, pp. 1437–1449, 1998.
- [14] R. W. Heath, S. Sandhu, and A. Paulraj, "Antenna selection for spatial multiplexing systems with linear receivers," *IEEE Communications Letters*, vol. 5, no. 4, pp. 142–144, 2001.
- [15] M. Gharavi-Alkhanjari and A. B. Gershman, "Fast antenna subset selection in MIMO systems," *IEEE Transactions on Signal Processing*, vol. 52, no. 2, pp. 339–347, 2004.
- [16] S. Sanayei and A. Nosratinia, "Antenna selection in MIMO systems," *IEEE Communications Magazine*, vol. 42, no. 10, pp. 68–73, 2004.
- [17] W. Yu, W. Rhee, S. Boyd, and J. M. Cioffi, "Iterative water-filling for Gaussian vector multiple-access channels," *IEEE Transactions on Information Theory*, vol. 50, no. 1, pp. 145–152, 2004.
- [18] W. Yu, W. Rhee, and J. M. Cioffi, "Optimal power control in multiple access fading channels with multiple antennas," in *Proceedings of the International Conference on Communications (ICC '01)*, pp. 575–579, June 2001.
- [19] Y. H. Pan, K. B. Letaief, and Z. Cao, "Dynamic spatial subchannel allocation with adaptive beamforming for MIMO/OFDM systems," *IEEE Transactions on Wireless Communications*, vol. 3, no. 6, pp. 2097–2107, 2004.
- [20] C. Masouros and E. Alsusa, "Two-stage transmitter precoding based on data-driven code-hopping and partial zero forcing beamforming for MC-CDMA communications," *IEEE Transactions on Wireless Communications*, vol. 8, no. 7, pp. 3634–3645, 2009.
- [21] C. Masouros and E. Alsusa, "Interference exploitation using adaptive code allocation for the downlink of precoded multiple carrier code division multiple access systems," *IET Communications*, vol. 2, no. 9, pp. 1118–1130, 2008.
- [22] C. Masouros and E. Alsusa, "Dynamic linear precoding for the exploitation of known interference in MIMO broadcast

- systems,” *IEEE Transactions on Wireless Communications*, vol. 8, no. 3, pp. 1396–1404, 2009.
- [23] P. Patel and J. Holtzman, “Analysis of a simple successive interference cancellation scheme in a DS/CDMA system,” *IEEE Journal on Selected Areas in Communications*, vol. 12, no. 5, pp. 796–807, 1994.
- [24] J. G. Proakis, *Digital Communications, Electrical Engineering*, McGraw-Hill, New York, NY, USA, 3rd edition, 1995.